IEEE Access
Multidisciplinary | Rapid Review | Open Access Journal

Received June 17, 2019, accepted June 19, 2019, date of publication July 1, 2019, date of current version July 19, 2019.

Digital Object Identifier 10.1109/ACCESS.2019.2925810

Instability of Gypsum Mining Goaf Under the Influence of Typical Faults

CONGRUI ZHANG[1,2], XUCHUN YANG[1,2], GAOFENG REN[1,2], BO KE[1,2], AND ZHANGLUN SONG[3]

[1]School of Resource and Environmental Engineering, Wuhan University of Technology, Wuhan 430070, China
[2]Key Laboratory of Mineral Resources Processing and Environment of Hubei Province, Wuhan University of Technology, Wuhan 430070, China
[3]Tongling Nonferrous Nanling Yaojialing Mining Company, Ltd., Wuhu 242400, China

Corresponding authors: Gaofeng Ren (rgfwhut@163.com) and Bo Ke (boke@whut.edu.cn)

This work was supported in part by the Natural Science Foundation of China under Grant 51774220, and in part by the Fundamental Research Funds for the Central Universities (WUT) under Grant 2019III187 and Grant 2019III083CG.

ABSTRACT Mine collapse is a common geological hazard associated with mining areas. In this paper, the goaf of a gypsum mine under the influence of typical faults is chosen as an example, and the stress on the center of the goaf roof is examined through theoretical analysis. The safety factors of the pillar at −127 m, −140 m, and −160 m are evaluated to be 1.471, 1.469, and 1.467, respectively, based on the Wilson theory. It is concluded that the structural parameters of the mining stope are reasonable without considering the influence of the fault. Furthermore, the numerical simulation by FLAC^{3D} is used to verify the analytical results and to study the influence of typical faults on the stress and displacement of the goaf. The results showed that the load of the roof and the pillars at a distance from the fault was larger than the load near the fault. First, the roof at this location is pulled. Next, cracks appear and develop. Then, the middle of the stope roof is pulled and falls, and the overburden strata move. Finally, the unstable strata are transmitted to the surface, and the ground surface of the mining area subsides.

INDEX TERMS Gypsum mine, typical fault, instability of goaf, finite difference method.

I. INTRODUCTION

In China, gypsum mines, most of which are common gypsum and anhydrite mines, have a large amount of storage and are widely distributed. The total storage of all kinds of gypsum mines is approximately 57 billion tons; thus, China ranks first in the world in terms of total gypsum mine storage [1]. However, because the pillars cannot perpetually retain stability, the sudden collapse of a large area of a gypsum mine goaf can occur.

The existing theory posits that the collapse of gypsum goafs is caused by the combined action of mining and geological factors. First, the open stope mining method results in a series of goafs with complex shapes. When the tensile strength of the goaf reaches its limit or the goaf undergoes external disturbances, the roof will suddenly break. The energy accumulated in the roof will be released to form a bump pressure with high intensity. Then, the overlapping goaf will collapse, resulting in large-scale mining disasters [2], [3]. Second, the special physical mechanical parameters of gypsum mines can cause hard roofs to fall within a very short time. If the gypsum deposit is affected by bad geological conditions at the same time, the ore body of its surrounding rock will be weakened, which increases the instability risk of the gob [4], [5].

The statistical data show that most of the bump pressure is directly related to faults. The main factors that induce bump pressure in faults include high structural stresses in faults, the occurrence of faults, the mechanical properties of rock in the surrounding fault zone and the degree of mining disturbance. The results indicate that, when the mining area is close to the crushed zone, because the roof is cut off and the force cannot be transferred, the roof will exert a great pressure on the pillars of the mining face and the fault. Then, a high stress concentration will be produced, resulting in a strong bump pressure with a large amount of energy [6]. Therefore, it is necessary to analyze the stress of goafs near the fault layer and the disturbance effect on the fault at different mining steps.

Yu *et al.* [7] constructed self-affine fractal curves and geological mining models with various kinds of fractal fault surfaces to simulate the mining-induced activation phenomenon

The associate editor coordinating the review of this manuscript and approving it for publication was Bora Onat.

of the fractal fault surface, and the law of the influence of the fractal fault surface on mining subsidence was studied and summarized. Wu *et al.* [8] used FLAC^{3D} to simulate and analyze the characteristics of mining stress evolution, fault activation patterns, and fault energy evolution characteristics. Islam and Shinjo [9] investigated the mining-induced reactivation of faults associated with the main conveyor belt roadway (CBR) of the Barapukuria Coal Mine in Bangladesh. The stress characteristics and deformation around the faults were investigated by the boundary element method (BEM) model. Sainoki and Mitri [10] investigated the influence of mining direction, i.e., overhand (bottom-up) versus underhand (top-down) mining, on the reactivation of a footwall fault in a sublevel stoping system. Jiang *et al.* [11] used UDEC to study the stress evolution of the working face and fault plane, the movement characteristics of overlying strata, and the law of fault slippage when the working face advanced from the footwall to the hanging wall according to the occurrence condition of a normal fault. Song *et al.* [12] suggested that the bump pressure of faults will occur only under certain lateral stress conditions. When the lateral pressure is low, the fault will slide stably without bump pressure. Li *et al.* [13] studied the mechanism of fault slippage inducing coal bumps under the influence of mining and suggested that, when the mining face is extended from the bottom of the fault to the fault, the risk of fault bump pressure will increase. Sherizadeh *et al.* [14] used the 3-dimensional distinct element analysis method to evaluate the effects of parameters such as the variation of the immediate roof rock mass strength properties, the variation in discontinuity mechanical properties, the orientations and magnitudes of the horizontal in situ stresses, and the size of pillars and excavations on the stability of the immediate roof.

Shuran and Shujin [15] chose comprehensive treatment solutions including subarea blasting caving and mine goaf closing by comparing programs and numerical simulations while also considering resource recycling to achieve safe, economic and highly effective conditions and lay the foundation for continued production. Wei [16] determined the grouting scope, the drilling space arrangement, the slurry and the treatment methods for common problems in construction and proposed ideas for building railways in the goafs to provide a reference for similar works. Liang *et al.* [17] evaluated the long-term stability of the rock strata above an old goaf and its possible impact on buildings above the rock strata, analyzed the releasable space in the strata and proposed a method for calculating this releasable space based on the characteristics of pore distribution in the rock strata above the goaf. Li [18] analyzed the factors affecting the stability of a goaf via site investigation, established a model of a goaf in the Yaogangxian mine based on numerical simulations, and suggested rational advice and suggestions for the control of potential safety hazards in the goaf of the Yaogangxian mine.

Most related research has been carried out for coal mines rather than gypsum mines. Because gypsum mines easily crack and have a higher hardness than coal mines, the above research results cannot fully reveal the collapse mechanism and influence range of gypsum mining goafs under the influence of faults.

While mining of the Longyuan Hengdian gypsum mine in Jingmen city, nine large goafs with an exposed area of 23,000 square meters were left at −127 m, −140 m and −160 m. A huge collapse from the goaf to the surface, which caused subsidence of the entire southern mining area, occurred in September 2014. The accident caused great economic losses and social impacts. In this work, based on this collapse, the influence of typical faults on the selection of the stope structural parameters was analyzed, and the mechanism of the influence of faults on the collapse of the remaining goafs was revealed.

II. ENGINEERING OVERVIEW

The Hengdian mining area of the Longyuan gypsum mine is located in the Hengdian village of the town of Macheng in the Yaodao district, 18 kilometers from Jingmen city. The parameters of two faults is are shown in Table 1, and mining method is an open-stope method. The parameters of the open-stope mining methods are shown in Table 2.

TABLE 1. Features of two faults and an ore body.

Feature name	F_1	F_2	Ore body
Tendency	240°	214°	240-260°
Dip angle	80°	120°	5-12°
Thickness	10~15m	20m ~ 40m	5.57m

TABLE 2. Mining parameters.

Feature name	value(m)
Length of stope (prone)	72.0
Width of stope (trend)	65.0
Length of stope room	57.0
Width of stope room	8.0
Width of pillar	4.5
Height of stope	4.5
Length of security pillar in the main transportation tunnel	8.0
Length of security pillar in the mining area	6.0

III. CALCULATION OF THE STRUCTURAL PARAMETERS OF THE STOPE UNDER THE INFLUENCE OF A FAULT

To calculate the stope structural parameters, it is necessary to first assess whether a new fault F_2 will cause damage. Then, we can determine the reasonable limit span of mining and calculate the safety factor for continuous pillars without considering the influence of a new fault F_2.

A. CALCULATION OF THE STABILITY OF THE GOAF

Two kinds of damage models are described in studies of the stability between faults and mining areas: those for disasters caused by instability under a relatively steady-state fault and those for disasters caused by instability under a dynamic fault. These two damage modes are based on the slippage damage of faults.

Therefore, fault slippage when establishing the mechanism of stope instability with faults must be determined.

The hypothesis of the theoretical analysis assumes the following: (a) the rock mass is homogeneous, and (b) the load comes from the mass of the upper strata.

The friction angle of the fault is φ, the dip angle of the fault is θ, the horizontal stress is T, and the vertical stress is V, as shown in Figure 1.

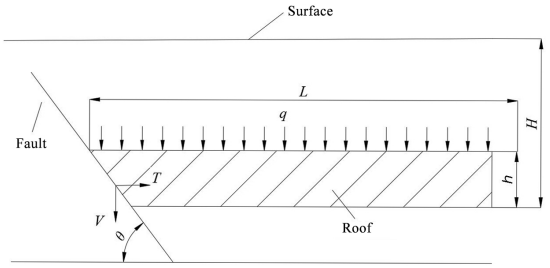

FIGURE 1. Analytical diagram of the roof stress under the influence of a fault.

According to the critical equation of the fault balance, when $V = \gamma H$ and $T = \lambda V = \lambda\gamma H$, the criterion of fault slip is obtained as Eq.(1). Thus, it can be seen that the fault slippage is only related to the lateral pressure coefficient of the rock mass

$$\tan\varphi = \frac{V\sin\theta + T\sin\theta}{T\sin\theta - V\sin\theta} = \frac{V+T}{T-V} = \frac{1+\lambda}{1-\lambda} \tag{1}$$

where λ is the coefficient of lateral pressure, γ is the bulk density, and H is the distance from the roof to the surface.

The lateral pressure coefficient of the rock mass can be obtained by the formula $\lambda = \frac{\upsilon}{1-\upsilon}$ [19], and the Poisson's ratio of gypsum ore is generally from 0.25 to 0.3. For the most unfavorable case, that is, $\upsilon = 0.25$, the lateral pressure coefficient will be 0.33 and the friction angle of the fault will be 30°, which is substituted into Eq. (1), to give:

$$\tan\varphi = \frac{\sqrt{3}}{3} < \frac{1+\lambda}{1-\lambda} = 1.98 \tag{2}$$

Therefore, fault F_2 will gradually slip and be further destroyed after the mining disturbance.

B. CALCULATION OF THE SPAN OF THE STOPE ROOM

According to the existing roof failure mechanism and material mechanics [20], the following formula can be obtained:

$$\sigma_{\text{Max tensile stress}} = \frac{\frac{3}{4}(2a)^2\rho_{\text{Original rock density}}}{L} \tag{3}$$

where a is half of the span, and L is the maximum limit falling height.

Then, Eq. (3) can be transformed to:

$$B = 2a = \sqrt{\frac{4}{3}\frac{L\times\sigma_{\text{Max tensile stress}}}{\rho_{\text{Original rock density}}}} \tag{4}$$

L is calculated by the empirical formula:

$$L = \frac{\rho_{\text{Stack height}} + \rho_{\text{Density at L}}}{2\rho_{\text{Original rock density}} - \rho_{\text{Stack heigh}} - \rho_{\text{Density at L}}} \times l \tag{5}$$

where l is the height of the goaf.

Given that the rocks on the pile surface are in a completely loose state in theory, the coefficient of looseness of the rock will be 1.3,which means:

$$\rho_{\text{Stack height}} = \frac{\rho_{\text{Original rock density}}}{1.3} \tag{6}$$

From the above formulas, it can be seen that, when $\rho_{Density\ at\ L}$ acquires the largest value, L will be the largest; and because $\rho_{Density\ at\ L}$ is smaller than $\rho_{Original\ rock\ density}$, when assuming $\rho_{Density\ at\ L}$ equals $\rho_{Original\ rock\ density}$, L would be the theoretical maximum value. Thus,

$$L = \left(\frac{1+1/1.3}{2-1-1/1.3}\right)\cdot l = 7.67l \tag{7}$$

Using Eq. (4), $\sigma_{Max\ tensile\ stress}$ equals 0.85 MPa and $\rho_{Original\ rock\ density}$ equals 2290 kg/m^3 according to the sample tests. Thus, the maximum length of the span can be calculated as follows:

$$B = \sqrt{\frac{4}{3}\times\frac{7.67l\times0.85\times10^6}{2290\times9.8}} = 19.68\sqrt{l} \tag{8}$$

Given that the real goaf roof is different from the theoretical model, the limit span of the multicrack rock mass is approximately 0.8–0.85 times the limit span of the noncrack rock mass. Thus, for a coefficient of 0.8:

$$B = 0.8\times19.68\sqrt{4.5} \approx 33m \tag{9}$$

During the mining process, goafs are ideally square or approximately square, and the maximum exposed area of a goaf is $\left[B/\sqrt{2}\right]^2$. Therefore, the maximum value of the exposed area is 544 m^2, while the actual stope length is 57 m, and the width of the stope cannot exceed 9.55 m. In the south mining area of the Hengdian gypsum mine, the stope span is generally 8 m; thus, it can be concluded that the structural parameters of the mine (the stope is 8 m in width and 57 m in length) are reasonable without considering fault F_2.

C. CALCULATION OF THE STABILITY OF PILLARS

Regarding pillar damage, the core area of the pillar is surrounded and restrained by the yield zone. The stress on the pillar gradually increases from the edge of the pillar to the center, and it finally reaches the failure strength at a certain distance, destroying the pillar. For most gypsum rocks, the damage stress in the core area is always approximately four times that of the lateral pressure, regardless of whether there is a lateral pressure limit around the rocks [21]. Because the lateral pressure is generally small and can be ignored, the damage strength F of the pillar rock in the core area is:

$$F = 4\sigma_3 \tag{10}$$

According to the distribution of the hydrostatic geological stress of gypsum ore, the initial geological horizontal stress of gypsum ore can be obtained as ρH, which is substituted into the above formula to give the damage strength $F = 4\rho H$. However, most underground gypsum ores have continuous pillars, and the bearing capacity limit of the section is [22]:

$$F = 4\rho Hp \tag{11}$$

where p is the width of the pillars.

Meanwhile, continuous pillars bear not only the direct load of the overburden rock directly above them but also the load from the surrounding rock extending from both sides of the stope [23], [24]. The load mechanical model is shown in the following diagram.

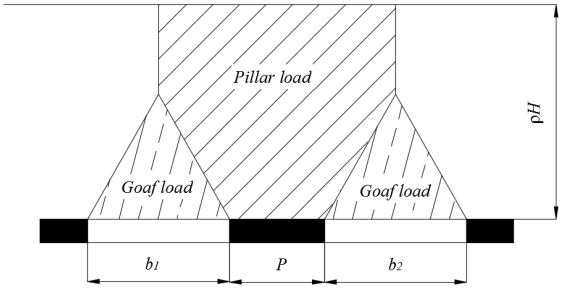

FIGURE 2. Analytical diagram of continuous pillar load.

From the mechanical distribution shown in Figure 2, it can be concluded that the load N produced by the pillar is:

$$\begin{aligned} \because N &= \rho\left[Hp + \frac{b_1}{4}(2H - \frac{b_1}{0.6}) + \frac{b_2}{4}(2H - \frac{b_2}{0.6})\right] \\ b_1 &= b_2 \\ \therefore N &= \rho\left[Hp + \frac{b}{2}(2H - \frac{b}{0.6})\right] \end{aligned} \tag{12}$$

The formula for the safety factor of the pillar is:

$$k = \frac{F}{N} = \frac{4\rho Hp}{\rho\left[Hp + \frac{b}{2}(2H - \frac{b}{0.6})\right]} \tag{13}$$

Therefore, if the mining thickness is 4.5 m and the width of the continuous pillar (stope pillar) is 4.5 m, the safety factor at −127 m can be calculated as:

$$\begin{aligned} k_{-127} &= \frac{F}{N} \\ &= \frac{4\times200\times2200\times4.5}{2200\times[200\times4.5+4\times(2\times200-8/0.6)]} = 1.471 \end{aligned}$$

Similarly, the safety factors of the other levels are $k_{-140} = 1.469$, $k_{-160} = 1.467$.

IV. FLAC^{3D} NUMERICAL SIMULATION

It can be seen from the above discussion that, without considering the influence of faults, the structural parameters of the stope in the mining area are reasonably designed by calculating the span length and width. However, the fault will occur by slip failure according to the calculation using the critical balance formula of the fault (Eq. (2)). Therefore, it can be assumed that the fault structure is the main cause of the collapse in the mining area. In this part, FLAC^{3D} is used for the numerical analysis of the instability accidents in the gypsum mining area with fault structures [25].

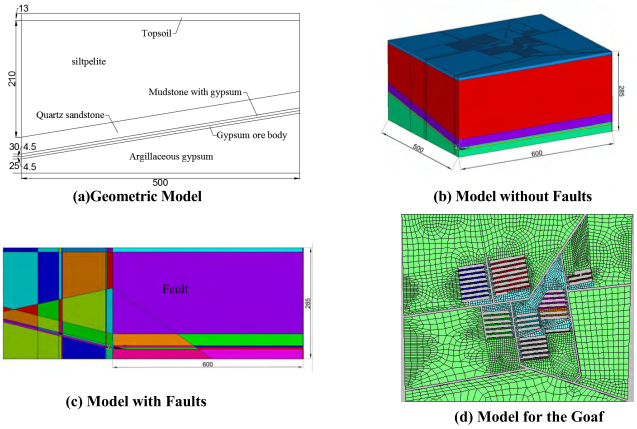

FIGURE 3. Model for Simulation.

A. ESTABLISHMENT OF THE MODEL

To reveal the influence of faults on the instability mechanism of the goaf, two kinds of numerical models are built, in which the length is 600 m, the width is 500 m, and the height is 285 m. Model A has no faults, and model B is constructed with five contact surfaces to build a three-dimensional model of the gypsum ore affected by the faults.

The material parameters are obtained from the previous rock mechanics experiment, and the detailed parameters are shown in Table 3.

The displacement boundary condition is used to restrict the boundary, which means that the displacement constraints are applied in the X direction, Y direction and bottom boundary of the model. In addition, the Mohr-Coulomb yielding criteria are adopted, and the 8-noded hexahedral solid element unit-Solit45 is used for simulation.

B. DISCUSSION

1) DISPLACEMENT

In simulations A and B, after completing the mining procedure, the displacement of the roof and floor of the stopes are shown in Figures 4 and 5, respectively. Figures 6 and 7 are displacement contour maps of each rock layer in the Z direction.

The following can be observed from Figures 4–7:

(1) Simulation A: The maximum settlement of the goaf roof in the Z direction is 1.85 cm, and the maximum rise of the goaf floor in the Z direction is 0.84 cm.

(2) Simulation B: The maximum settlement of the goaf roof in the Z direction is 0.8 cm, which is obtained on the surrounding rocks, and the maximum rise of the goaf floor in the Z direction is 1.0 cm, which is found in the floor and the surrounding rocks of the stopes.

TABLE 3. Physical and mechanical parameters of rock mass.

Rock formation name	Dry bulk density (kg/m^3)	Bulk modulus (GPa)	Shear modulus (GPa)	Friction angle (°)	Cohesion (MPa)	Tensile strength (MPa)	Compressive strength (MPa)
Topsoil	1800	1.00	0.10	20	0.04	0.15	--
Silt mudstone	2190	0.83	0.18	20	3.35	0.34	4.00
Quartz sandstone	2360	1.02	0.47	28	2.72	1.01	8.74
Gypsum ore	2290	3.33	1.11	30	8.25	0.85	10.49
Mud in the bottom	2160	3.08	0.88	28	3.30	1.02	8.50

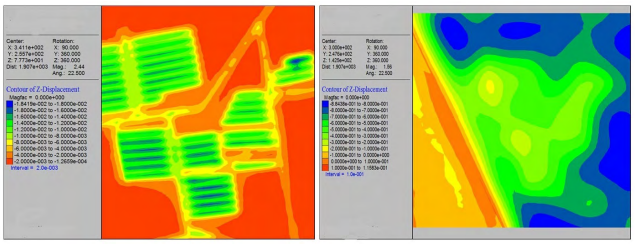

(a) Simulation A (b) Simulation B

FIGURE 4. Displacement of the roof in the Z direction.

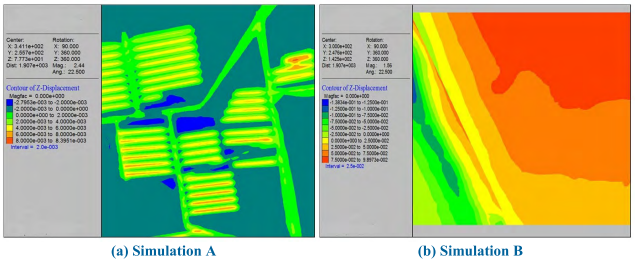

(a) Simulation A (b) Simulation B

FIGURE 5. Displacement of the floor in the Z direction.

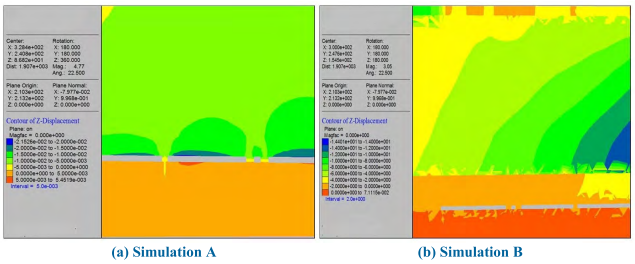

(a) Simulation A (b) Simulation B

FIGURE 6. Displacement of each rock layer in the Z direction (parallel strike of the ore body).

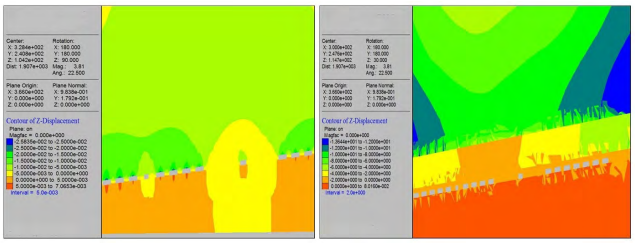

(a) Simulation A (b) Simulation B

FIGURE 7. Displacement of each rock layer in the Z direction (vertical strike of the ore body).

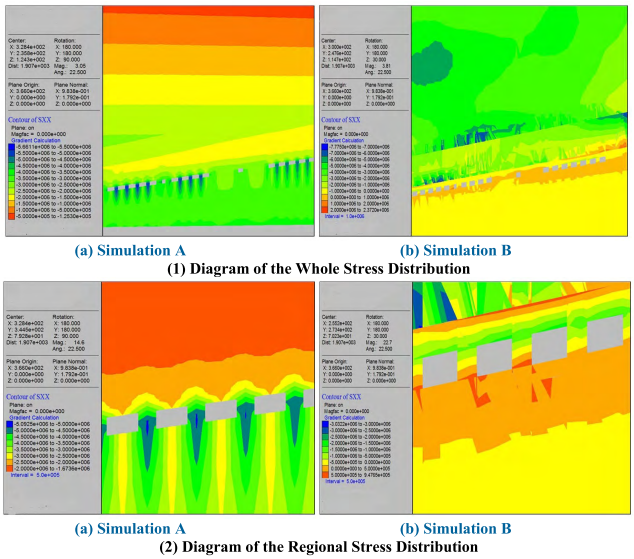

(a) Simulation A (b) Simulation B

(1) Diagram of the Whole Stress Distribution

(a) Simulation A (b) Simulation B

(2) Diagram of the Regional Stress Distribution

FIGURE 8. Diagram of the stress distribution for σ_{xx}.

(3) The risk to the goaf is increased under the influence of faults. At the same time, the subsidence of overlying strata and the surface is far larger than that of the areas affected by faults. The closer the stope is to the fault, the more conspicuous the displacement of the roof and floor.

(4) The displacement begins at both sides of the fault in opposite directions. Then, the faults slip, and the roof settlement and the floor rise near the faults increase. Therefore, it can be deduced that the floor has collapsed, and separation has occurred in the roof and the overlying strata.

2) STRESS

The stress distributions of the mining area in the two simulations are shown in Figures 8–10.

The following can be observed from Figures 8–10:

(1) Simulation A: Under the influence of mining, the strata near the goaf show reduced stress, while the strata near the

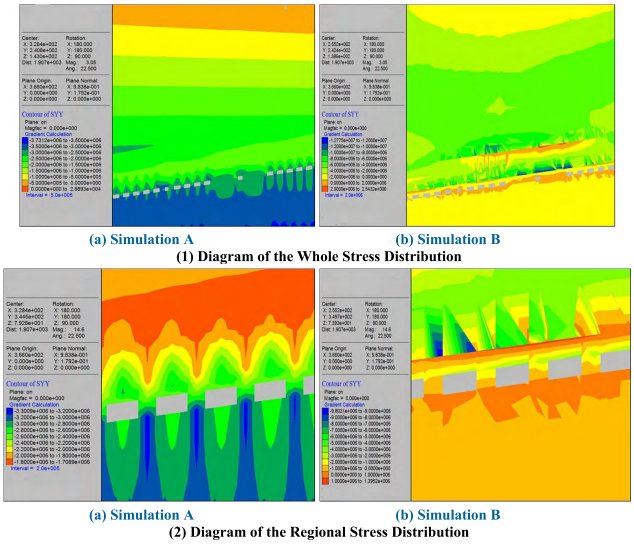

FIGURE 9. Diagram of the stress distribution for σ_{yy}.

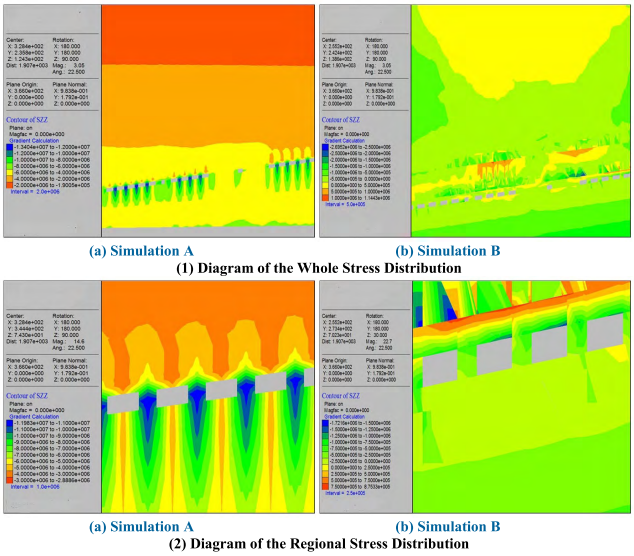

FIGURE 10. Diagram of the stress distribution for σ_{zz}.

pillar show increased stress. In the pillar, the maximum horizontal stress σ_{xx} is approximately -5.1 MPa, σ_{yy} is approximately -3.4 MPa, and the maximum vertical stress σ_{zz} is approximately -12.1 MPa. If the stress in the pillar exceeds the limit compression strength of the gypsum ore body, then the pillar will be destroyed.

(2) Simulation B: Under the influence of both fault failure and chamber stoping, the maximum stress occurs in the surrounding rocks, especially in the sand roof. Nevertheless, the stress is not obvious in the roof, the floor or the pillar of goaf. The stress distribution near the fault increases gradually, and the maximum horizontal stress σ_{xx} of the roof and pillar is approximately -4.5 MPa, σ_{yy} is approximately -7.0 MPa, and the maximum vertical stress σ_{zz} is approximately -17.2 MPa. Additionally, tension stresses appear in the rocks. The roof of the mining area is destroyed from the direction close to the fault inclination, and the stress in the roof exceeds the ultimate compressive strength of the gypsum ore body, which will lead to roof collapse.

(3) The stress near the fault concentrates, causing the stress concentration area to shift toward the fault. For the pillar, the pillar near the fault has been greatly damaged and can no longer transmit the upload stress to the rock layer below. Meanwhile, the support force on the pillar far from the fault is greater than that near the fault. Thus, the stress where the roof and pillar contact increases and damage occurs, while the roof of the stope falls and collapses due to the impact pressure, and the entire mining area collapses. In addition, the stress of the roof and the pillar near the fault increases, and the risk also increases.

3) PLASTIC ZONE

The distributions of the plastic zones from the goaf roof, gypsum ore and goaf floor are shown in Figures 11–13, respectively.

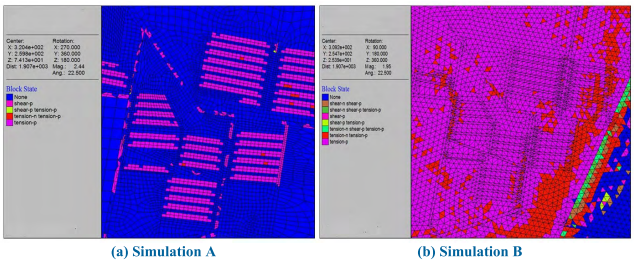

FIGURE 11. Distribution of the plastic zone on the roof.

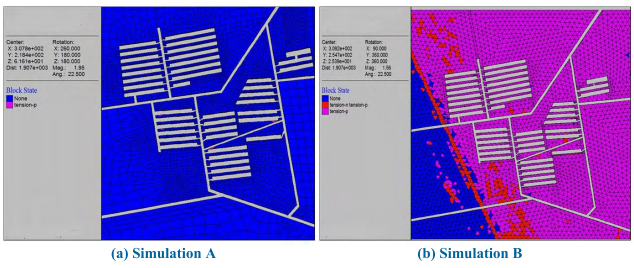

FIGURE 12. Distribution of the plastic zone of gypsum ore.

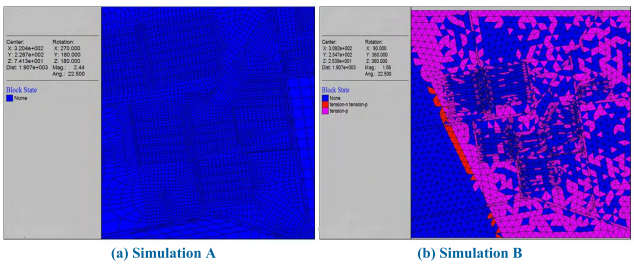

FIGURE 13. Distribution of the plastic zone on the floor.

The following can be observed from Figures 11–13:

(1) Simulation A: Plastic damage occurs in the goaf, and most of the damage is tensile damage, which mainly destroys

the goaf roof in the middle of the mining area. Plastic damage, which is tensile damage, also occurs in the gypsum ore, and the damage mainly occurs in the security pillar near the side of the roadway. Meanwhile, no plastic damage occurs in the goaf floor of the mining area.

(2) Simulation B: Plastic damage, most of which is tensile failure and shear damage, occurs in a large area of the roof in the mining area. The tensile damage is mainly distributed near the fault and the upper part of the mining area. Shear failure is mainly distributed in the footwall of the fault. The floor of the mining area also suffered varying degrees of tensile damage, mainly distributed near the upper wall of the fault.

(3) It can be observed from the comparative analysis of case A and case B that the area of the plastic zone affected by the fault in the stope roof and floor is much larger than that of the plastic zone without fault, and the fault blocks the upward spreading of the plastic zone. Tensile damage and shear damage are first produced in the fault and then spread toward the mining area near the fault, which will damage the goaf roof and floor by tension failure. Then, a series of collapse phenomena occurred in the ore chamber along the dip direction of the ore body.

V. CONCLUSION

From the research on the instability mechanism of gypsum mining goafs under the influence of faults, the following conclusions are reached based on theoretical analysis and numerical simulation:

(1) A model for roof stress analysis is built, and the safety factors of pillars at different levels are obtained to verify the rationality of the structural parameters of the stope without considering fault F_2. It is theorized that the instability of the goaf in Hengdian gypsum mine is caused by faults in the area.

(2) FLAC^{3D} is used to simulate the instability of the mining goaf in the Hengdian gypsum mine. The results show that the plastic zone of the mining area terminates at the fault, and the displacement and stress also changed suddenly at the fault. Thus, the fault structure blocks the extension of the plastic zone and the transmission of stress and displacement. The displacement and damage of the roof and the pillars that are 30–40 m from the fault are notably larger than the area farther from or closer to the fault, and the subsidence of the whole mining area spreads from nearer locations to farther locations. Thus, the faults impact the stability of the goaf.

(3) By comparing the results of the theoretical analysis and the numerical simulation, it has been proven that the instability accidents in the goaf are caused by the newly discovered slippage of fault F_2.

(4) The development rule of goaf instability under the influence of faults can be described as follows. First, the roof far from the fault produces tensile failure and cracks. Then, the middle of the roof is damaged by tensile failure, and thus, the roof falls and the overburdened strata move. Finally, the instability is transmitted to the surface, the ground surface will sink, and a floor heave will appear at the center of the goaf roof.

DATA AVAILABILITY

The data used to support the findings of this study are available from the corresponding author upon request.

CONFLICTS OF INTEREST

The authors declare that there are no conflicts of interest regarding the publication of this paper.

REFERENCES

[1] *Information Center of Ministry of Land and Resources of China, World Mineral Resources Annual Review (2016)*, Inf. Center Ministry Land Resour. China, Geological Publishing House, Beijing, China, 2017.

[2] H. Luan, H. Lin, and Y. Jiang, "Risks induced by room mining goaf and their assessment: A case study in the shenfu-dongsheng mining area," *Sustainability*, vol. 10, no. 3, p. 631, Feb. 2018. doi: 10.3390/su10030631.

[3] H. Li, B. Zhao, G. Guo, J. Zha, and J. Bi, "The influence of an abandoned goaf on surface subsidence in an adjacent working coal face: A prediction method," *Bull. Eng. Geol. Environ.*, vol. 77, no. 1, pp. 305–315, Feb. 2018. doi: 10.1007/S10064-016-0944-9.

[4] G.-F. Ren, H.-Y. Yang, S.-S. Zhang, J.-L. Lv, and Z.-L. Song, "On the propagation rules and safety precautions of the air shock waves caused by the roof caving in gypsum mine gob," *J. Saf. Environ.*, vol. 15, no. 6, pp. 86–91, Dec. 2015. doi: 10.13637/j.issn.1009-6094.2015.06.017.

[5] G.-C. He, D.-X. Ding, Y. Liu, and Z.-J. Zhang, "ANFIS prediction of the surface subsidence of the old goaf of the gypsum mine in hengshan," *J. Mining Saf. Eng.*, vol. 29, no. 6, pp. 876–881, Nov. 2012.

[6] J.-P. Zuo, Z.-H. Chen, H.-W. Wang, X.-P. Liu, and Z.-P. Wu, "Experimental investigation on fault activation pattern under deep mining," *J. China Coal Soc.*, vol. 34, no. 3, pp. 305–309, Mar. 2009. doi: 10.13225/j.cnki.jccs.2009.03.006.

[7] Y. Guangming, Z. Jianfeng, and X. Heping, "Numerical simulation of fractal interface effect of mining-caused activation of fault," *Discrete Dyn. Nature Soc.*, vol. 7, no. 3, pp. 151–155, Jan. 2002. doi: 10.1080/1026022021000001418.

[8] Q.-S. Wu, L.-S. Jiang, and Q.-L. Wu, "Study on the law of mining stress evolution and fault activation under the influence of normal fault," *Acta Geodynamica Geomaterialia*, vol. 14, no. 3, pp. 357–369, Sep. 2017. doi: 10.13168/AGG.2017.0018.

[9] M. R. Islam and R. Shinjo, "Mining-induced fault reactivation associated with the main conveyor belt roadway and safety of the Barapukuria Coal Mine in Bangladesh: Constraints from BEM simulations," *Int. J. Coal Geol.*, vol. 79, no. 4, pp. 115–130, Sep. 2009. doi: 10.1016/j.coal.2009.06.007.

[10] A. Sainoki and H. S. Mitri, "Influence of mining activities on the reactivation of a footwall fault," *Arabian J. Geosci.*, vol. 10, no. 5, p. 99, Feb. 2017. doi: 10.1007/s12517-017-2913-4.

[11] J.-Q. Jiang, P. Wang, L.-S. Jiang, P.-Q. Zheng, and F. Feng, "Numerical simulation on mining effect influenced by a normal fault and its induced effect on rock burst," *Geomech. Eng.*, vol. 14, no. 4, pp. 337–344, Mar. 2018. doi: 10.12989/gae.2018.14.4.337.

[12] Y. Song, S. Ma, X. Yang, and Y. Jiang, "Experimental investigation on instability transient process of fault rockburst," *Chin. J. Rock Mech. Eng.*, vol. 30, no. 4, pp. 812–817, Apr. 2011.

[13] Z. H. Li, L. M. Dou, A. Y. Cao, J. Fan, and Z. L. Mu, "Mechanism of fault slip induced rockburst during mining," *J. China Coal Soc.*, vol. 36, no. 1, pp. 68–73, May 2011. doi: 10.13225/j.cnki.jccs.2011.s1.024.

[14] T. Sherizadeh and P. Kulatilake, "Assessment of roof stability in a room and pillar coal mine in the U.S. using three-dimensional distinct element method," *Tunnelling Underground Space Technol.*, vol. 59, pp. 24–37, Oct. 2016. doi: 10.1016/j.tust.2016.06.005.

[15] L. V. Shuran and L. Shujin, "Research on governance of potential safety hazard in Da'an mine goaf," *Procedia Eng.*, vol. 26, pp. 351–356, Dec. 2011. doi: 10.1016/j.proeng.2011.11.2178.

[16] Y.-H. Wei, "Research on reinforcement of foundation in coal mine goaf for Guangxi coastal railway," *J. Railway Eng. Soc.*, vol. 178, no. 7, pp. 6–10 and 46, Jul. 2013.

[17] L. Li, K. Wu, and D.-W. Zhou, "Evaluation theory and application of foundation stability of new buildings over an old goaf using longwall mining technology," *Environ. Earth Sci.*, vol. 75, no. 9, p. 763, May 2016. doi: 10.1007/s12665-016-5574-9.

[18] L. Feng, "Research on control of potential safety hazard in goaf of yaogangxian Tungsten mining," *J. Saf. Sci. Technol.*, vol. 10, no. 9, pp. 152–157, Sep. 2014. doi: 10.11731/j.issn.1673-193x.2014.09.026.
[19] C. Li and S. Zhu, "On misunderstandings of the rock lateral pressure coefficient," *J. Southwest Petroleum Univ. (Sci. Technol. Ed.)*, vol. 39, no. 3, pp. 135–140, Jun. 2017. doi: 10.11885/j.issn.1674-5086.2015.10.26.01.
[20] J.-A. Wang, X.-C. Shang, H. Liu, and Z.-Y. Hou, "Study on fracture mechanism and catastrophic collapse of strong roof strata above the mined area," *J. China Coal Soc.*, vol. 33, no. 8, pp. 850–855, Aug. 2008. doi: 10.3321/j.issn:0253-9993.2008.08.003.
[21] H. Xu, Y. Wang, and A. Wu, "Instability risk evaluation of insulating pillar of excavation in depth based on comprehensive index method," *Nonferrous Metals Eng.*, vol. 8, no. 1, pp. 98–104, Feb. 2018. doi: 10.3969/j.issn.2095-1744.2018.01.020.
[22] T. Kostecki and A. J. S. Spearing, "Influence of backfill on coal pillar strength and floor bearing capacity in weak floor conditions in the Illinois Basin," *Int. J. Rock Mech. Mining Sci.*, vol. 76, pp. 55–67, Jun. 2015. doi: 10.1016/j.ijrmms.2014.11.011.
[23] H. Bingnan, "Stability analysis of the pillar in strip mining," *J. China Coal Societ*, vol. 20, no. 2, pp. 205–210, Apr. 1995. doi: 10.13225/j.cnki..jccs.1995.02.020.
[24] X. Cui and X. Miao, "Analysis of stresses acting on strip pillar and form of subsidence curve," *J. China Univ. Mining Technol.*, vol. 29, no. 4, pp. 52–55, Jul. 2000.
[25] S. Dehghan, K. Shahriar, P. Maarefvand, and K. Goshtasbi, "3-D numerical modelling of Domino failure of hard rock pillars in Fetr6 Chromite Mine, Iran, and comparison with empirical methods," *J. Central South Univ.*, vol. 20, no. 2, pp. 541–549, Feb. 2013. doi: 10.1007/s11771-013-1517-8.

CONGRUI ZHANG was born in Wuhan, Hubei, China, in 1991. He received the B.S. and M.S. degrees in mining engineering from the Wuhan University of Technology, where he is currently a Researcher. His research interests include rock mechanics and mining methods.

XUCHUN YANG was born in Qin'an, Gansu, China, in 1995. He received the B.S. degree in mining engineering from the Wuhan University of Technology, Wuhan, China, where he is currently pursuing the M.S. degree. His research interests include rock mechanics and mining methods.

GAOFENG REN received the B.S., M.S., and Ph.D. degrees in mining engineering from the Wuhan University of Technology, where he is currently a Professor. His work has been funded by grants from the Natural Science Foundation of China and the National Key Research and Development Plan. His research interests include mining methods, disaster control technology, safety evaluation, and rock behavior in cold regions.

BO KE received the B.S. and M.S. degrees in mining engineering from the Wuhan University of Technology, Wuhan, China, and the Ph.D. degree in mining engineering from Central South University. He is currently an Academic Lecturer with the Wuhan University of Technology. His research interests include mining methods, borehole stability, and rock mechanics.

ZHANGLUN SONG was born in 1989. He received the M.S. degree in mining engineering from the Wuhan University of Technology, Wuhan, China. He is currently a Vice Minister of the Technology Department, Tongling Nonferrous Nanling Yaojialing Mining Company, Ltd.